Journal of Science and Technology
ISSN: 2456-5660, Volume 4, Issue 3, May-June 2019, PP 01-13
www.jst.org.in

Performance comparison between conventional and modified Range Doppler Algorithm in real time applications

I. Hemalatha[1]*, P. V. Sridevi[2]
[1]*Sir C R Reddy College of Engineering, Eluru,* Department of ECE, h*emacrr2006@gmail.com*
[2]*AndhraUniversity,College of Engineering(A),Visakhapatnam, Department of ECE, pvs6_5@yahoo.co.in*
**corresponding author*

Abstract: *Synthetic aperture radar is an active remote sensing approach that transmits the known wavelength signal and measures the reflected wave from the scene. Moving target detection, imaging, and velocity estimation using raw data are active research fields with civilian and military applications. The synthetic aperture radar endures from the image degradation because of phase errors present in the received signal. These phase errors give rise to poor focus quality, spurious targets, loss of resolution and erroneous velocities. The primary objective of the paper is to produce a high-resolution image of the targets and the moving targets motion estimation present in the scene in the presence of phase errors. The modified range-Doppler algorithm performs the range migration correction and the focus filtering with the wavelet decomposition to improve the resolution of the target image. The parameters extracted from the range migration correction and azimuth filtering is used to estimate the moving target velocity. The modified RDA using Sym8 wavelet decomposition levels with AOPM for moving target velocity estimation of SAR image have the average percentage of accuracy is 1.99. This proposed RDA method gives the close approximation to the actual velocity value and also improves the focus quality of the target image when compared with the conventional RDA.*
Keywords : *Synthetic aperture radar, Range Doppler algorithm, Wavelet decomposition.*

I. Introduction

Velocity estimation of moving targets is one of the important research topics in SAR imaging. The moving target in the scene is first focused well before velocity estimation. The range Doppler algorithm [1], [2] is used to focus the moving targets in SAR imaging. The range migration correction [5] and focus filtering [4] is performed in RDA. For further improving the focus quality we proposed modified range Doppler algorithm. The wavelet decomposition levels are used in the modified RDA for improvement of the focus quality after azimuth compression.

The moving target velocity in SAR imaging is composed of two components i.e. the cross-track velocity and the along-track velocity. The coefficient extracted from the range migration correction is used to calculate the accurate Doppler centroid. The radial velocity of the moving target is estimated from the Doppler centroid. The coefficient extracted from the azimuth filtering is used to calculate the moving target along-track velocity. The adaptive order polynomial method and the phase gradient method are used for azimuth filtering. The performance of the modified RDA is compared with the performance of the conventional RDA. The focus quality of the moving target in the scene is measured by using the parameter entropy. The paper is organized as follows: Section 1 deals with the introduction. Section 2 presents automatic imaging of moving target in SAR imaging. The radial velocity and the cross-range velocity estimation is discussed in section 3. Section 4 and section 5 contains results and conclusions respectively.

2. Automatic imaging

Motion parameters of moving target are extracted from its automatic imaging. The flowchart of proposed modified Range Doppler Algorithm for SAR imaging is as shown in Fig. 1.

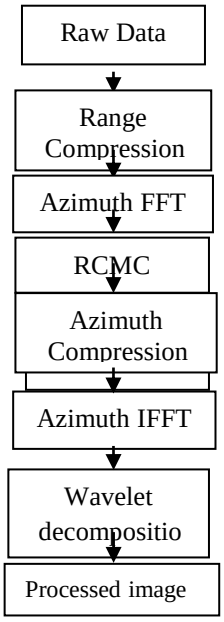

Fig. 1 Block diagram of Modified Range-Doppler algorithm.

First, the received echo signals from the scaterrers are resolved in fast time using their different time delays and the range resolution is improved using matched filtering the received signals with range reference signal. Similarly, the signals from scaterrers are resolved in slow time based on their different azimuths and the azimuth resolution is improved using focus filter. To acquire well focused and a correct positioned image, range migration correction before azimuth filtering, and wavelet decomposition after azimuth filtering is required. The range migration correction, azimuth filtering and wavelet decomposition are performed automatically during imaging of the moving target.

2.1 Range cell migration correction

The range between the target and the radar is varied because the target is moving through the azimuth antenna beam; the echoes from the same target are not placed in the same range bin. It exhibit very poor focus quality of the image. The range migration correction is carried out in the range-Doppler domain, the echoes returned from the particular target are placed at corresponding range bin. The range migration correction is accomplished by shifting the samples at a Doppler frequency in the range Doppler domain up to the amplitudes are equal. This is referred to as automatic range migration correction.

2.2 Focus filtering

The focus filter minimizes the phase errors present in received signal and improves the focus quality of image by matched filtering the columns of Fourier transformed RCMC signal with the azimuth reference signal in azimuth direction. The design of the azimuth filter is based on the received echo signal from the moving target. This is known as autofocus. The phase gradient method [12] is used to estimate the phase errors present in the received signal. The focus filter coefficient is adjusted to design the phase response; therefore the sharpness of the image is optimized.

2.3 Wavelet decomposition

After azimuth compression, a de-noised azimuth compression signal is obtained by using wavelet coefficients thresholding using global positive threshold THR [10, 28-31]. Haar, Db4, and Sym8 wavelets with 2, 4, & 6 decomposition levels are used to reduce the noise. Noise due to the phase errors are further reduced by this process.

3. Velocity estimation

The received reflected wave from the object is represented as:

$$x(t) = w \exp(-j\frac{4\pi r(t)}{\lambda}) \quad (1)$$

Where t is slow time, w is the parameter of scattering, λ is the carrier wavelength and $r(t)$ is the distance between the detector and the object. Here $r(t)$ is written as:

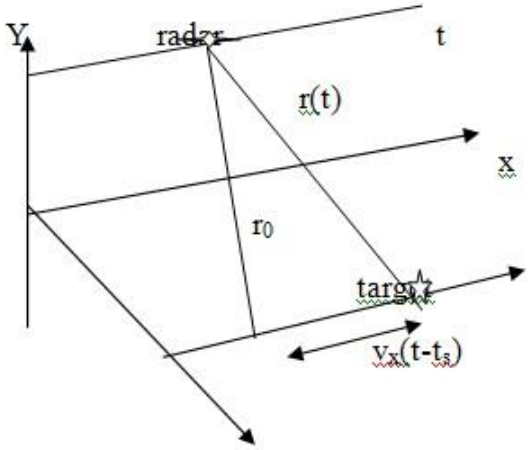

Fig. 2 Graphical representation of SAR imaging plane

$$r(t) = \sqrt{\left(y_o + v_y t - V_y t\right)^2 + (x_o + v_x t - V_x t)^2} \quad (2)$$

and it is derived from the SAR imaging plane shown in above Fig. 2. Let us consider the y-axis is the radar bore sight directed towards target. The radar moves with radial velocity V_y in y-axis and cross range velocity V_x in x-axis. Let the target also moves with radial velocity v_y and with cross range velocity v_x. At t=0, the target is located at point (x_0, y_0) and the radar at point (0, 0).

After some time$t = t_s$ the radar bore sight is directed to the target, therefore:

$$t_s = \frac{x_0}{V_x - v_x} \quad (3)$$

and r_0 be the range of the scatter to the radar at t_s is given by:

$$r_o = y_o + v_y t_s - V_y t_s \quad (4)$$

Then, approximating the r(t) by its second order Taylor series at t_s , we obtain:

$$r(t) = r_o - (V_y - v_y)\ (t - t_s)\ +\ \frac{(V_x - v_x)^2}{2r_0}(t - t_s)^2 \tag{5}$$

substituting above equation (5) into equation (1) yields:

$$x(t) = w\ exp\left\{-j\frac{4\pi}{\lambda}\left[r_o - \left(V_Y - v_y\right)(t - t_s) + \frac{(V_y - v_y)}{2r_o}(t - t_s)^2\right]\right\} \tag{6}$$

Differentiate the phase angle of x(t) will results the instantaneous Doppler frequency of that received signal i.e.:

$$\Omega_i = \frac{4\pi}{\lambda}\left[\left(V_y - v_y\right) - \frac{(V_x - v_x)^2}{r_o}(t - t_s)\right] \tag{7}$$

An important parameter called Doppler centriod can be defined as Doppler shift of a target; it is located in the antenna bore sight direction.

Doppler centriod is obtained by substituting $t = t_s$ in above eq...(7):

$$\Omega_o = \frac{4\pi}{\lambda}\ (V_y - v_y) \tag{8}$$

$$t - t_s = -\frac{\lambda r_o}{4\pi(V_x - v_x)^2}(\Omega_i - \Omega_o) \tag{9}$$

substituting equation (9) into (5) yields:

$$r(t) = r_o + \frac{\lambda r_o(V_y - v_y)}{4\pi(V_x - v_x)^2}(\Omega_i - \Omega_o) + \frac{\lambda^2 r_o}{32\pi^2(V_x - v_x)^2}(\Omega_i - \Omega_o) \tag{10}$$

Equation (10) exhibits the relationship between the distance and the instantaneous Doppler frequency. This gives the approximate relationship between spectral Doppler frequency and range. Therefore the shifting of the Doppler slice in the range is given as

$$r_o - r(t) = -\frac{\lambda r_o(V_y - v_y)}{4\pi(V_x - v_x)^2}(\Omega_i - \Omega_o) - \frac{\lambda^2 r_o}{32\pi^2(V_x - v_x)^2}(\Omega_i - \Omega_o) \tag{11}$$

Extending the equation (11) to the original interval and discretizing $r_\Omega = r_o - r(t)$ and Ω_i , we get:

$$r(k) = \begin{cases} -\sum_{i=1}^{2}\alpha_i\left[\frac{2}{M}(k - k_o)\right]^i, 0 \le k < k_o + \frac{M}{2} \\ -\sum_{i=1}^{2}\alpha_i\left[\frac{2}{M}(k - k_o - M)\right]^i, k_o + \frac{M}{2} \le k < M \end{cases} \tag{12}$$

$$\alpha_1 = \frac{\lambda r_o (V_y - v_y)}{4dT(V_x - v_x)^2} \quad (13)$$

$$\alpha_2 = \frac{\lambda^2 r_o}{32dT^2(V_x - v_x)^2} \quad (14)$$

where index of instantaneous Doppler frequency Ω_i is k, fast time sampling period is d, the shifting of the samples at a Doppler frequency k is $r(k)$ and normalized by d. the coefficients of range cell migration are α_1 and α_2.

The azimuth filter phase response is properly designed to improve the sharpness of the image. For azimuth compression, the design of the azimuth filter phase response with the parameters, that depends upon the radar velocity, the pulse repetition frequency (PRF), and the absolute range.

The azimuth filter phase response is derived as follows,

The Fourier transform of the received echo signal x(t) is approximately equal to:

$$x(\Omega_i) = w\sqrt{\frac{\lambda r_o}{2(V_x - v_x)^2}}\ exp\left[-j\frac{\pi}{4} - j\frac{4\pi}{\lambda}r_o - j\Omega_i t_s + j\frac{\lambda r_o}{8\pi(V_x - v_x)^2}(\Omega_i - \Omega_o)^2\right] \quad (16)$$

The azimuth filter phase response should be:

$$\phi(\Omega_i) = -\frac{\lambda r_o}{8\pi(V_x - v_x)^2}(\Omega_i - \Omega_o)^2 \quad (17)$$

Extending the equation (16) to the original period and discretizing $\phi(\Omega_i)$, Ω_i and model as polynomial i.e.:

$$\phi(k) = \begin{cases} -\sum_{i=2}^{I} \pi\beta\left(\frac{k-k_o}{M}\right)^i, 0 \le k < k_o + \frac{M}{2} \\ -\sum_{i=2}^{I} \pi\beta\left(\frac{k-k_o-M}{M}\right)^i, k_o + \frac{M}{2} \le k < M \end{cases} \quad (18)$$

$$\beta = \frac{\lambda r_o}{2T^2(V_x - v_x)^2} \quad (19)$$

The phase response $\phi(k)$ of azimuth filter with k as independent parameter and β is called the parameter of azimuth filter.

Focus filter parameter β is adjusted to minimize the phase errors present in azimuth compression signal to improve the sharpness of the focused image and it is referred to as the autofocus. Minimum entropy autofocus using phase gradient method carried out in the following way.
Focus filtering is achieved by:

$$P(m,n) = \frac{1}{M}\sum_{k=0}^{M-1} x_r(k,n)\ exp\big(j\phi(k)\big) \quad (20)$$

Doppler rate, azimuth, and fast time are indexed by k, m and n, respectively. The range cell migration corrected signal is $x_r(k,n)$, and the phase response of azimuth filter is Φ(k). P (m, n) is the complex image. The focus quality of complex image P (m, n) is improved by reducing phase errors of focus filter. The phase response Φ(k) of azimuth filter is optimized until the entropy of $|P(m,n)|^2$ is minimized.

The entropy of $|P(m,n)|^2$ is defined as:

$$\varepsilon[|P(m,n)|^2] = \sum_{m=0}^{M-1}\sum_{n=0}^{N-1}\frac{|P(m,n)|^2}{S} ln\frac{S}{|P(m,n)|^2} \quad (21)$$

Where $S = \sum_{m=0}^{M-1}\sum_{n=0}^{N-1}|P(m,n)|^2$

In SAR imaging, the entropy can be used to measure the smoothness of a distribution function, using this characteristic of entropy, sharpness of an image to be calculated [9-14].The entropy of $|P(m,n)|^2$is minimized implies phase errors of focus filter are reduced, and focus quality of complex image is improved.

Let the focus filter's amplitude response is assumed to be a unit and S is a constant. Therefore the entropy of image can be determined by:

$$\varepsilon[|P(m,n)|^2] = -\sum_{m=0}^{M-1}\sum_{n=0}^{N-1}|P(m,n)|^2 ln|P(m,n)|^2 \quad (22)$$

Thus, the entropy of image has to be minimized by estimating the phase response of the azimuth filer

3.1 Estimation of Φ(k) using phase gradient method

Estimation of Φ(k) is depending upon the parameter βi. To improve the computational efficiency, the signal is focused using conventional focus filter and de-noised using wavelet decomposition. From the de-noised signal, the parameter β is adjusted as follows.

Phase estimation and correction

Phase Gradient method is used to estimate phase errors present in the azimuth compression signal. The first step in the PGM is to select strongest scatter from each range bin and shift it to the origin, to remove the frequency offset due to the Doppler of the target. Circular shifting is used for this process. The next important step is windowing the circularly shifted image data. The gradient of phase error estimation from circularly shifted and windowed image data is given by:

$$g(u)=\frac{\sum_{n=0}^{N}\mathrm{Im}\left\{G^{*}{}_{n}(u)G_{n}(u)\right\}}{\sum_{n=0}^{N}\left|G_{n}(u)\right|^{2}} \quad (23)$$

filter coefficient β relation with Doppler rate where g(u) is the gradient of the phase error, $G_n(u)$ is the inverse Fourier transform of the circularly shifted and windowed azimuth compression image data. The slope rate of the gradient of phase errors is estimated and then the variance of Doppler rate df_r is calculated. Therefore the Doppler rate fr is equal to $f_r + df_r$ and the azimuth filter coefficient $\beta = \frac{1}{T^2 f_r}$. According to phase errors in azimuth compression signal, β is adjusted to get fine focused SAR target image.

3.2 Estimation of Φ(k) using Adaptive-order polynomial autofocus method

Estimation of $\phi(k)$ depends upon the parameter β_i. The conventional focus filtering is taking place before autofocus to improve computational efficiency. First β_2 is increased step by step until entropy ε [.] is

minimized. If Ɛ [.] cannot be minimized β_2 is varied in the opposite direction until the entropy of image Ɛ [.] is minimized. This process is repeated for β_3, β_4 and so on until Ɛ [.] is minimized. The phase response $\phi(k)$ is adjusTABLE, if further increase in order, the estimate of β_i approaches to zero and therefore the higher order terms are not considered, because the estimates of two successive β_i are equal to zero.

The focus quality of image is measured by entropy. Better focus corresponds to smaller entropy. After calculating β, the RCMC coefficient is determined by dividing equations 13 by 19:

$$\alpha_1 = \left(V_y - v_y\right)\frac{\beta T}{2d} \tag{24}$$

RCMC, focus filtering and wavelet decomposition is carried out automatically until entropy is minimized. From these coefficients the radial and cross-range velocities are estimated. The radial velocity is represented by $v_y = V_y - \frac{2d\alpha_1}{\beta T}$ and the cross-range is given by $v_x = V_x - \frac{1}{T}\sqrt{\frac{\lambda r_o}{2\beta}}$. The total velocity of moving target is estimated by using the parameters cross-track velocity 'v_y' and the along-track velocity 'v_x' is written as:

$$v = \sqrt{\left[\frac{V_y}{\cos(\theta)}\right]^2 + {v_x}^2} \tag{25}$$

4. Results

The detector moves at a cross-track velocity of 0.262m/s and along-track velocity of 7125m/s. 0.56ms is the radar pulse repetition period. The beam has an angle of 0 rad in azimuth. The wavelength of pulses has 5.67 cm and 15.5MHz bandwidth. 1.896 MHz is the sampling frequency, and 1024 pulses with 512 fast time samples each are recorded. When the azimuth time is 0, the detector is located at (0, 0) and the center of the object located at (0, 1547300km). Fig. 3 shows the moving car with velocity about 5m/s at the airport [23]. The image of the car in the scene is blurred because of its motion. The car image is isolated from the stationary background using MATLAB command 'roipoly' and converted into signal. This signal is processed for automatic image formation and for velocity estimation using modified RDA and conventional RDA.

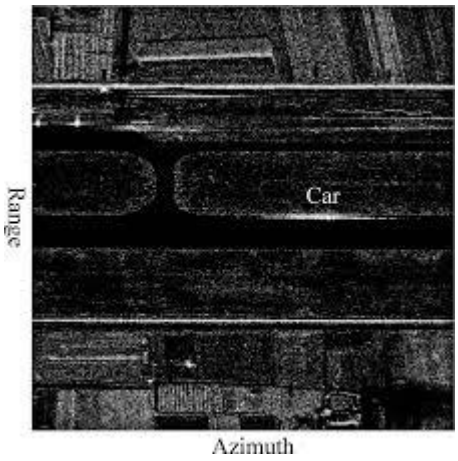

Fig. 3 Moving car image at airport

TABLE-1

Car velocity estimation using conventional RDA
True velocity of car = 5m/s

S. No	Method		Radial velocity (m/s)	Cross-range velocity (m/s)	Estimated velocity (m/s)	Velocity error (m/s)
1	Conventional RDA	PGA	-1.4860	-4.3564	4.6028	0.3972
		AOPM	-1.4860	-4.7528	4.9796	0.0203

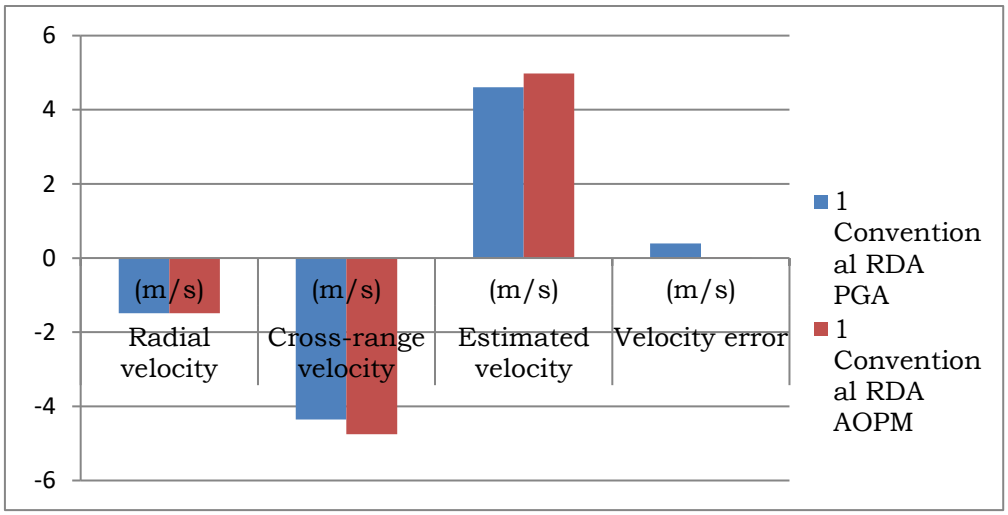

Fig 4 Estimation of car velocity using conventional RDA with PGA and AOPM.

TABLE-1 and Fig 4 show the car velocity estimation using conventional RDA with PGA and with AOPM. 0.3972m/s and 0.0203m/s are the velocity errors using PGA and AOPM respectively. According to the observations, 7.94% and 0.4% accuracy is obtained for PGA and AOPM respectively. AOPM performs better when compared with PGA.

TABLE-2
Car velocity estimation using modified RDA with Haar de-composition
True velocity of car = 5m/s

S. No	Modified RDA		Radial velocity (m/s)	Cross-range velocity (m/s)	Estimated velocity (m/s)	Velocity error (m/s)
1	Haar-2L decomposition	PGA	-1.4060	-5.0435	5.2518	0.2518
		AOPM	-1.4660	-4.7565	4.9956	0.0043
2	Haar-4L decomposition	PGA	-1.4660	-5.0435	5.2522	0.2522
		AOPM	-1.4060	-5.1453	5.3497	0.3497
3	Haar-6L decomposition	PGA	-1.4060	-5.1287	5.4371	0.4371
		AOPM	-1.4660	-4.9491	5.1793	0.1793

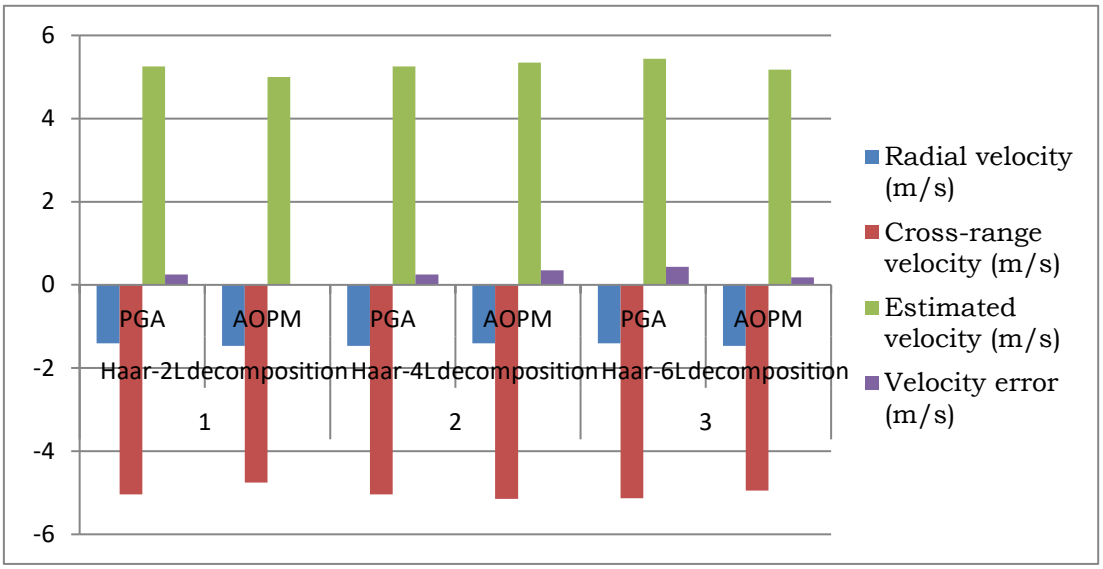

Fig 5 Estimation of car velocity using modified RDA with Haar decomposition levels

TABLE-2 and Fig 5 show the estimation of car velocity using modified RDA with Haar decomposition levels using PGA and AOPM. 6.3% and 3.5% average accuracy is obtained from PGA and AOPM respectively. AOPM with Haar decomposition performs better when compared with PGA.

TABLE-3
Car velocity estimation using modified RDA with Db4 de-composition
True velocity of car = 5m/s

S. No	Modified RDA		Radial velocity (m/s)	Cross-range velocity (m/s)	Estimated velocity (m/s)	Velocity error (m/s)
1	Db4-2L decomposition	PGA	-1.4060	-5.1287	5.3337	0.3337
		AOPM	- 1.4660	-4.6546	4.8987	0.1012
2	Db4-4L decomposition	PGA	-1.4860	-4.4713	4.7316	0.2683
		AOPM	-1.4660	-5.2509	5.4684	0.4684
3	Db4-6L decomposition	PGA	-1.4060	-3.8435	4.1130	0.8869
		AOPM	-1.4860	-4.0509	4.2452	0.7547

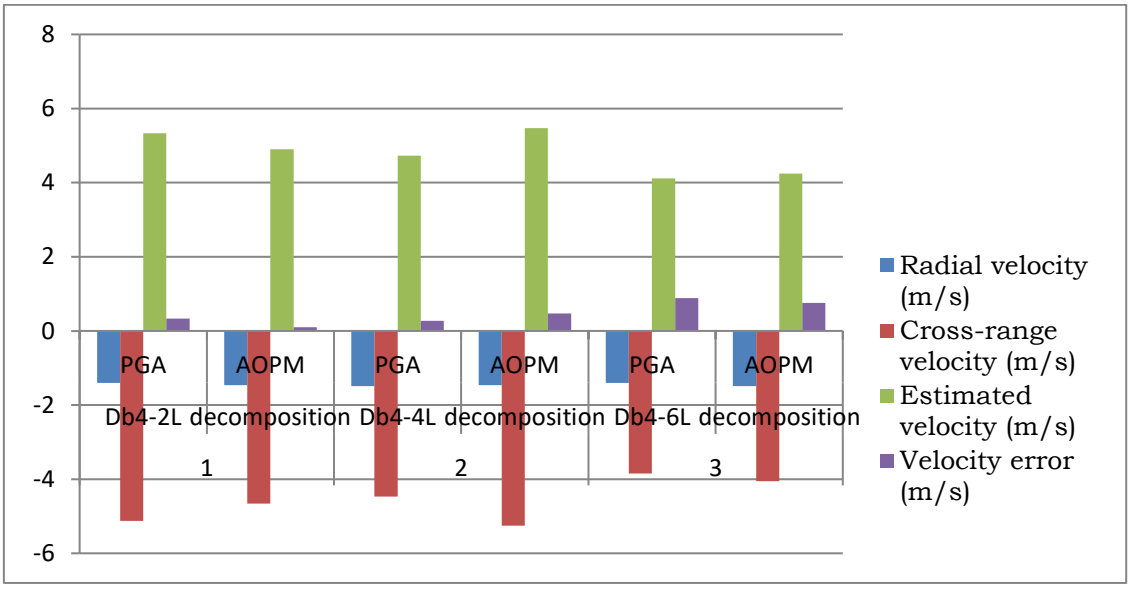

Fig 6 Estimation of car velocity using modified RDA with Db4 decomposition levels.

TABLE-3 and Fig 6 show the estimation of car velocity using modified RDA with Db4 decomposition levels using PGA and AOPM. 9.9% and 8.8% average accuracy is obtained from PGA and AOPM respectively. AOPM with Db4 decomposition performs better when compared with PGA.

TABLE-4
Car velocity estimation using modified RDA with Sym8 de-composition
True velocity of car = 5m/s

S. No	Modified RDA		Radial velocity (m/s)	Cross-range velocity (m/s)	Estimated velocity (m/s)	Velocity error (m/s)
1	Sym8-2L decomposition	PGA	-1.4860	-4.7861	4.9516	0.0483
		AOPM	-1.4860	-4.7454	4.9914	0.0085
2	Sym8-4L decomposition	PGA	-1.4660	-5.0139	5.2412	0.2412
		AOPM	-1.4260	-4.8509	5.0732	0.0732
3	Sym8-6L decomposition	PGA	-1.4060	-4.8713	5.0867	0.0867
		AOPM	-1.4060	-4.5528	4.7825	0.2174

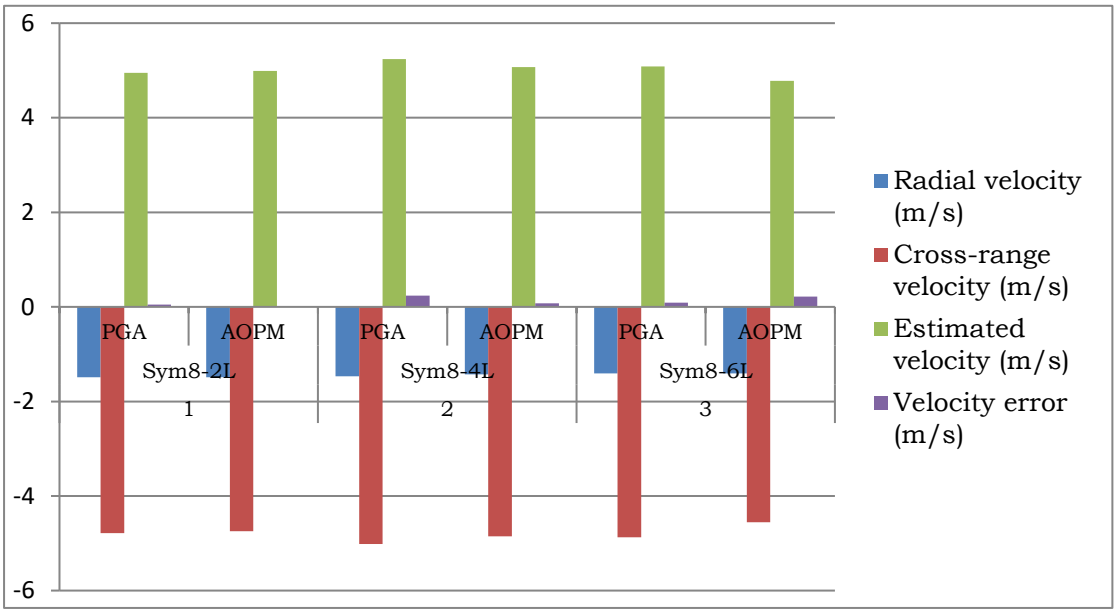

Fig 7 Estimation of car velocity using modified RDA with Sym8 decomposition levels.

TABLE-4 and Fig 7 show the estimation of car velocity using modified RDA with Sym8 decomposition levels using PGA and AOPM. 2.5% and 1.99% average accuracy is obtained from PGA and AOPM respectively. AOPM with Sym8 decomposition performs better when compared with PGA.

5. Conclusions

Modified and conventional RDA with PGA and AOPM is used for car velocity estimation in SAR imaging. 1.99% average accuracy is obtained by using modified RDA with Sym8 decomposition levels using AOPM. This value is less than when compared to the remaining methods. Therefore AOPM with Sym8 performs better for SAR real data when compared with the other existing methods.

References

[1] Curlander, J.C., and McDonough, R.N.," Synthetic Aperture Radar: systems and signal processing". New York, NY: John Wiley & Sons, 1991.

[2] R.K.Raney, H.Runge, R.Bamler, G.Cumming,, and F.H.Wong., 'Precision SAR Processing Using Chirp Scaling',IEEE Transactions on Geoscience, remote Sens., vol.32, no.4,pp.786-799 ,july. 1994

[3] R.Bamler, "Acomparison of range-doppler and wave number
domain SAR focusing algorithms". IEEE Transactions on Geosci, remote Sens., vol.30, no.4,pp.706- 713,jul.1992

[4] Wang,J., and Liu,X., "SAR minimum-entropy autofocus using an adaptive – order Polynomial model". IEEE Geoscience and Remote Sensing Letters, 3, 4(oct,2006),512-516

[5] Wang,J., and Liu,X.,"Automatic correction of range migration in SAR Imaging".IEEE Geoscience and Remote Sensing Letters,7. 2(Apr,2010),256-260.

[6] Wang,J., and Liu,X., " Velocity estimation of moving targets in SAR imaging".IEEE Transactions on Aerospace and Electronic System,50. 2(Apr,2014),1543-1548.

[7] Caner Ozdemir, "Inverse Synthetic Aperture Radar Imaging With Matlab Algorithms". Wiley Series In Microwave And Optical Engineering.

[8] Y.K.Chan and V.C.Koo , "An Introduction To Synthetic Aperture Radar (SAR)".

[9] Bhuvan, Indian Geo-platform of ISRO

[10] Michel Misiti., Yves Misiti., Georges Oppenheim., Jean-Michel Poggi Wavelet Toolbox, For Use With MATLAB

[11] P. H. Eichel, D. C. Ghiglia, and C. V. Jakowatz, "Speckle processing method for synthetic aperture radar phase correction," Opt. Lett., vol. 14, no. 1, pp. 1–5, Jan. 1989.

[12] D. E. Wahl, P. H. Eichel, D. C. Ghiglia, and C. V. Jakowatz, "Phase gradient autofocus—A robust tool for high resolution SAR phase correction," IEEE Trans. Aerosp. Electron. Syst., vol. 30, no. 3, pp. 827–835, Jul. 1994.

[13] S. Barbarossa and A. Farina, "A novel procedure for detecting and focusing moving objects with SAR based on the Wigner-Ville distribution," in Proc. IEEE Int. Radar Conf., 1990, pp. 44–50.

[14] Y. G. Niho, "Phase difference auto focusing for synthetic aperture radar imaging," U.S. Patent 4999635, Mar. 12, 1991.

[15] E. A. Herland, "Seasat SAR processing at the Norwegian Defense Research Establishment," in Proc. EARSeL-ESA Symp., 1981, pp. 247–253.

[16] R. P. Bocker, T. B. Henderson, S. A. Jones, and B. R. Frieden, "A new inverse synthetic aperture radar algorithm for translational motion compensation," Proc. SPIE, vol. 1569, pp. 298–310, 1991.

[17] X. Li, G. Liu, and J. Ni, "Autofocusing of ISAR images based on entropy minimization," IEEE Trans. Aerosp. Electron. Syst., vol. 35, no. 4, pp. 1240–1251, Oct. 1999.

[18] D. Kasilingam, J. Wang, J. Lee, and R. Jensen, "Focusing of synthetic aperture radar images of moving targets using minimum entropy adaptive filters," in Proc. IEEE Int. Geosci. and Remote Sens. Symp., 2000, pp. 74–76.

[19] J. R.Fienup and J. J. Miller, "Aberration correction by maximizing generalized sharpness metrics," J. Opt. Soc. Amer. A, Opt. Image. Sci., vol. 20, no. 4, pp. 609–620, Apr. 2003.

[20] J. Wang, X. Liu, and Z. Zhou, "Minimum-entropy phase adjustment for ISAR," Proc. Inst. Elect. Eng., Radar, Sonar Navigat., vol. 151, no. 4, pp. 203–209, Aug. 2004.

[21] J. Wang and X. Liu, "SAR minimum-entropy autofocus," in Proc. Int. Radar Conf., 2004.

[22] I. Hemalatha, P. V. Sridevi., "Optimization of phase response of focus filter in sar imaging". IJAERD, Vol. 5, no. 4, April -2018.

[23] X. Wang, R. Wang, N. Li, H. Fan, and Y. Wang, "A method of estimating the velocity of moving targets for use in high-resolution wide-swath SAR imaging," *Remote Sens. Lett.*, vol. 9, no. 4, pp. 305–313, Apr. 2018.

[24] T. Jin, X. Qiu, D. Hu, and C. Ding, "An ML-Based Radial Velocity Estimation Algorithm for Moving Targets in Spaceborne High-Resolution and Wide-Swath SAR Systems," *Remote Sens.*, vol. 9, no. 5, p. 404, Apr. 2017.

[25] W. Weiwei, Z. ShengQi, Z. Jie Jie, and L. Guisheng, "Compressive sensing-based ground moving target indication for dual-channel synthetic aperture radar," *IET Radar Sonar Navig.*, vol. 7, no. 8, pp. 858–866, Oct. 2013.

[26] Min Lei, Yu Yang, XiaoMing Liu, MingZhi Cheng, and Rui Wang, "Audio zero-watermark scheme based on discrete cosine transform-discrete wavelet transform-singular value decomposition," *China Commun.*, vol. 13, no. 7, pp. 117–121, Jul. 2016.

[27] H. Demirel and G. Anbarjafari, "IMAGE Resolution Enhancement by Using Discrete and Stationary Wavelet Decomposition," *IEEE Trans. Image Process.*, vol. 20, no. 5, pp. 1458–1460, May 2011.

[28] T. Celik and T. Tjahjadi, "Image Resolution Enhancement Using Dual-Tree Complex Wavelet Transform," *IEEE Geosci. Remote Sens. Lett.*, vol. 7, no. 3, pp. 554–557, Jul. 2010.

[29] H. Demirel, C. Ozcinar, and G. Anbarjafari, "Satellite Image Contrast Enhancement Using Discrete Wavelet Transform and Singular Value Decomposition," *IEEE Geosci. Remote Sens. Lett.*, vol. 7, no. 2, pp. 333–337, Apr. 2010.

[30] M. Z. Iqbal, A. Ghafoor, and A. M. Siddiqui, "Satellite Image Resolution Enhancement Using Dual-Tree Complex Wavelet Transform and Nonlocal Means," *IEEE Geosci. Remote Sens. Lett.*, vol. 10, no. 3, pp. 451–455, May 2013.